Disclinated states in nematic elastomers

Eliot Fried & Russell E. Todres

Department of Theoretical and Applied Mechanics
University of Illinois at Urbana-Champaign
Urbana, IL 61801-2935, USA

We present a theory for uniaxial nematic elastomers with variable asphericity. As an application of the theory, we consider the time-independent, isochoric extension of a right circular cylinder. Numerical solutions to the resulting differential equation are obtained for a range of extensions. For sufficiently large extensions, there exists an isotropic core of material surrounding the cylinder axis where the asphericity vanishes and in which the polymeric molecules are shaped as spherical coils. This region, corresponding to a disclination of strength +1 manifesting itself along the axis, is bounded by a narrow transition layer across which the asphericity drops rapidly and attains a non-trivial negative value. The material thereby becomes anisotropic away from the disclination so that the polymeric molecules are shaped as ellipsoidal coils of revolution oblate about the cylinder radius. In accordance with the area of steeply changing asphericity between isotropic and anisotropic regimes, a marked drop in the free-energy density is observed. The boundary of the disclination core is associated with the location of this energy drop. For realistic choices of material parameters, this criterion yields a core on the order of 10^{-2} μm, which coincides with observations in conventional liquid-crystal melts. Also occurring at the core boundary, and further confirming its location, are sharp transitions in the behavior of the constitutively determined contribution to the deformational stress and a minimum in the pressure. Furthermore, the constitutively determined contribution to the orientational stress is completely concentrated at the core boundary. The total energy definitively shows an energetic preference for disclinated states.

1. Introduction

As technological applications of liquid crystals have grown over the past thirty years, so too has research into the structure and importance of their defects. Initially, defect-induced disruptions were the bane of liquid crystal displays. Now, though, these very defects are being harnessed in the zenithal bistable display, which unlike traditional LCD displays, does not require sustained power to retain an image (Mottram and Sluckin 2000). Also, the presence of defects is necessary for the stabilization of some of the blue phases observed in cholesteric liquid crystals, wherein the regular three-dimensional lattice is actually composed of disclination lines (Chandrasekhar 1988; Kléman 1989). In addition, recent research has shown the important effect of disclinations on the reduction of the nematic-isotropic phase transition temperature in nematic liquid-crystals (Mottram and Sluckin 2000; Mottram and Hogan 1997).

Liquid crystals serve as an exemplar of a class of materials ideally suited for the study of defects. Since point, line, and surface defects manifest themselves in liquid crystals, their study has also had far-reaching consequences on the field of defects in disordered systems, frustrated media, convective instabilites, and biological molecules. For example, biological polymers such as DNA, PBLG, and xanthan exhibit textures, most of whose defects are similar to those observed in cholesteric liquid crystals (Kléman 1989).

Submitted to *Journal of the Mechanics and Physics of Solids*

A disclination in a nematic liquid-crystal is a line along which the director is undefined. In the Oseen–Zöcher–Frank (OZF) theory (Oseen 1933; Zöcher 1933; Frank 1958), a non-integrable singularity in the free-energy density occurs at a disclination. Initially, this difficulty was addressed by positing a core of fixed radius and energy about the disclination. However, the fixed energy approach gives no information about the magnitude and energy of the core and also fails to elucidate the underlying physical nature of the core (Ericksen 1991; Mottram and Hogan 1997). Nevertheless, for nematics confined to capillaries, it has been shown that the director can 'escape into the third dimension' at the singularity, thus obviating the need for a core but not ruling one out altogether (Williams et al. 1972). This deficiency of the OZF theory led Ericksen (1991) to develop a regularized theory involving the degree-of-orientation, a scalar field which vanishes at disclinations and enters the free energy density in a manner that mollifies the singularity otherwise associated with a disclination. Exploiting this idea, researchers have obtained values of the core radius and energy of a disclination in a cylindrical configuration (Adrienko and Allen 2000; Mottram and Hogan 1997; Mottram and Sluckin 1997).

Here, we study disclinations in nematic elastomers. These materials differ from melts in that the polymer chains are cross-linked. As in a melt, the nematic mesogens may still be either main-chain or pendant. Our motivation for this investigation rests on the aforementioned importance of defects in nematic melts and recent research into these novel materials (Anderson et al. 1999; Davis 1993; DeSimone and Dolzmann 2000; Finkelmann, et al. 2001; Warner and Terentjev 1996; Zentel 1989).

We confine our attention to uniaxial nematic elastomers. In such materials, the agglomeration of polymer chains is described completely by a scalar asphericity $q > -1$ and a unit orientation $\boldsymbol{n}$. For $-1 < q < 0$, the chains are oblate about $\boldsymbol{n}$, spherical for $q = 0$, and prolate about $\boldsymbol{n}$ for $q > 0$. Supplemental to the deformation $\boldsymbol{y}$, which describes the distortion of the cross-links forming the network, q and $\boldsymbol{n}$ have the status of additional kinematic degrees of freedom in our theory. Consistent with the rubbery nature of nematic elastomers, we require that the deformation be isochoric.

For simplicity, we ignore inertial, thermal, and compositional effects. To take account of changes in the asphericity, we introduce *aspherical forces* which expend power over the time-rate of the asphericity and stipulate that these forces comply with an *aspherical force balance* which we impose in addition to the more conventional (Anderson et al. 1999) balances for deformational force, orientational force, and moments. Within our purely mechanical setting, the first and second laws of thermodynamics are enforced through an *energy imbalance*.

We consider a constitutive theory in which the independent variables are the deformation gradient, the asphericity, the asphericity gradient, the orientation, the orientation gradient, and the asphericity rate. The approach taken by Anderson et al. (1999) yields thermodynamically-based restrictions on the constitutive relations, reducing the constitutive description of a nematic elastomer to the provision of the free-energy density and a scalar drag coefficient.

Next, we consider a nematic elastomer that is formed by a two-step process and specialize our theory accordingly. Specifically, we suppose that the melt is cross-linked in a uniaxial state with a certain ellipsoidal agglomeration. Then, we presume that the elastomer is annealed, giving rise to an isotropic reference state in which the agglomeration at each material point is spherical. We assume that

the material retains "memory" of the asphericity at the time of cross-linking but that the annealing process destroys completely the orientation associated with this asphericity. This naturally leads us to propose a specific form for the free-energy density, a simultaneous extension and simplification of the molecular-statistical expression of Warner, Gelling and Vilgis (1988). This free-energy density includes contributions associated with the distortion of network cross-links, the asphericity of the molecular agglomeration, and the orientation of the axis of the molecular agglomeration. The aspherical contributions include a term that accounts for the memory of the asphericity present at the time of cross-linking and a term quadratic in the gradient of the asphericity which allows for the existence of equilibrium states in which the asphericity varies smoothly between its energetically preferred values. The orientational contribution includes terms that can be related to the classical splay, twist, bend, and saddle-splay terms of the OZF theory but accounts as well for interactions between the deformation of the network and the orientation of the molecular agglomeration.

Finally, we apply the theory to a simple example problem: the static extension of a right circular cylinder. In approaching this problem, we prescribe the deformation and assume that, wherever it is defined, the orientation vector is always in the radial direction. Under these circumstances, the problem reduces to a boundary-value problem—parameterized by the extension ratio of the cylinder—for the asphericity.

We obtain numerical solutions to this boundary-value problem for different extension ratios of the cylinder. For sufficiently large extensions, there exists an isotropic core of material surrounding the cylinder axis where the asphericity vanishes and in which the polymeric molecules are shaped as spherical coils. This region corresponds to the existence of a disclination of strength $+1$ along the axis and is bounded by a narrow transition layer across which the asphericity drops rapidly and attains a non-trivial negative value. The material thereby becomes anisotropic away from the disclination so that the polymeric molecules are shaped as ellipsoidal coils of revolution oblate about the cylinder radius. For realistic choices of the material parameters, we find that the disclination core radius is on the order of 10^{-2} μm and, thus, coincident with observations in conventional liquid-crystalline melts.

Using the solutions obtained for the asphericity, we plot the contribution to the free-energy density by various groupings of its component terms. We observe that the free-energy density has a markedly different behavior within and without the core region, which confirms our initial estimate of the core radius.

We then use the solutions to compute the non-trival components of the consitutively determined contributions to the deformational and orientational stresses as functions of the radial coordinate. For all three non-trivial components of the constitutively determined contribution to the deformational stress, we observe a sharp transition in behavior at the core boundary. Interestingly, the radial component within the core region decreases with increasing extension. Additionally, we note a similar trend for the hoop component outside of the core. We also study the pressure distribution across the domain. For all extension ratios, the pressure is a montonically decreasing function from the cylinder's center to the core boundary, where it reaches a minimum. From there to the cylinder's edge, it increases monotonically, although with a much more gentle slope than the decreasing part. As one might expect, across the domain, the pressure is higher for greater extension ratios. Further, we find that the single non-trivial component of the constitutively deter-

mined contribution to the orientational stress is exclusively concentrated about the core boundary.

We also investigate the total energies of both the core region and the entire cylinder. We find that the energy of the cylinder shows an expected monotonic increase with increasing cylinder elongation. Importantly, for our whole range of extension, the total energy is always less than the classical elastic energy which the material would possess if it were to remain isotropic. This clearly indicates that the disclinated state is preferred. Focusing only on the core, the proportion of total energy contained there increases with increasing extension for almost our entire range and then drops slightly. This trend indicates that the core becomes energetically more influential at greater extension levels.

2. Kinematics

We consider an incompressible nematic elastomer which, in a reference state, occupies a region $\mathcal{R}$ in a three-dimensional space $\mathcal{E}$. At each point $\boldsymbol{x}$ of $\mathcal{R}$, we envision a cross-linked network of polymeric molecules which include nematic mesogens as main-chain elements or as pendant side-groups. We assume that the material is free of preferred alignment, and thus isotropic in the reference state.

In general, the kinematic state of a nematic elastomer is described by two fields:

- the *deformation* $\boldsymbol{y}$, a time-dependent mapping of $\mathcal{R}$ into $\mathcal{E}$, which serves as a macroscopic measure of the distortion of the network cross-links; and
- the *agglomeration* $\boldsymbol{A}$, a time-dependent mapping of $\mathcal{R}$ into the set of symmetric and positive-definite tensors, which serves as a macroscopic measure of the nematically-induced distortion of the molecules comprising the network.

We confine our attention to situations where the agglomeration has the uniaxial form

$$\boldsymbol{A} = (1+q)^{\frac{1}{3}}\Big(\boldsymbol{1} - \frac{q}{1+q}\boldsymbol{n}\otimes\boldsymbol{n}\Big), \tag{2.1}$$

in which the *asphericity* q and the *orientation* $\boldsymbol{n}$ obey

$$q > -1 \qquad \text{and} \qquad |\boldsymbol{n}| = 1. \tag{2.2}$$

For $-1 < q < 0$, $\boldsymbol{A}$ describes an oblate ellipsoid of revolution about $\boldsymbol{n}$. In the case $q = 0$, $\boldsymbol{A}$ describes a sphere, while for that of $q > 0$, $\boldsymbol{A}$ describes a prolate ellipsoid of revolution about $\boldsymbol{n}$.

We use Grad to denote differentiation on $\mathcal{R}$ and, in particular, write

$$\boldsymbol{F} = \operatorname{Grad}\boldsymbol{y}, \qquad \boldsymbol{G} = \operatorname{Grad}\boldsymbol{n}, \qquad \text{and} \qquad \boldsymbol{h} = \operatorname{Grad} q \tag{2.3}$$

for the gradients of $\boldsymbol{y}$, $\boldsymbol{n}$, and q. Further, we use a superposed dot to indicate partial-differentiation with respect to time.

Since the medium is incompressible, we require that the deformation be isochoric, viz.,

$$\det \boldsymbol{F} = 1. \tag{2.4}$$

3. Basic laws

We formulate the basic laws in the referential setting, using $\mathcal{P}$ to designate an arbitrary, regular part of $\mathcal{R}$ with boundary $\partial\mathcal{P}$ oriented by a unit normal field $\boldsymbol{\nu}$ directed outward from $\mathcal{P}$.

For simplicity, we ignore all forms of inertia and external force.

(*a*) *Deformational force balance*

We introduce a *deformational stress* $\boldsymbol{S}$ that arises in response to changes in $\boldsymbol{y}$ and impose deformational force balance by requiring that

$$\int_{\partial\mathcal{P}} \boldsymbol{S}\boldsymbol{\nu}\, da = \boldsymbol{0} \tag{3.1}$$

for all $\mathcal{P}$ and all time, or, equivalently, that

$$\operatorname{Div}\boldsymbol{S} = \boldsymbol{0} \tag{3.2}$$

on $\mathcal{R}$ for all time.

(*b*) *Aspherical force balance*

We introduce an *aspherical stress* $\boldsymbol{\tau}$ and an *internal aspherical force density* k that act in response to changes in q and impose aspherical force balance by requiring that

$$\int_{\partial\mathcal{P}} \boldsymbol{\tau}\cdot\boldsymbol{\nu}\, da + \int_{\mathcal{P}} k\, dv = 0 \tag{3.3}$$

for all $\mathcal{P}$ and all time, or, equivalently, that

$$\operatorname{Div}\boldsymbol{\tau} + k = 0 \tag{3.4}$$

on $\mathcal{R}$ for all time.

(*c*) *Orientational force balance*

We introduce an *orientational stress* $\boldsymbol{\Sigma}$ and an *internal orientational force density* $\boldsymbol{\pi}$ which act in response to changes in $\boldsymbol{n}$ and impose orientational force balance by requiring that

$$\int_{\partial\mathcal{P}} \boldsymbol{\Sigma}\boldsymbol{\nu}\, da + \int_{\mathcal{P}} \boldsymbol{\pi}\, dv = \boldsymbol{0} \tag{3.5}$$

for all $\mathcal{P}$ and all time, or, equivalently, that

$$\operatorname{Div}\boldsymbol{\Sigma} + \boldsymbol{\pi} = \boldsymbol{0} \tag{3.6}$$

on $\mathcal{R}$ for all time.

(*d*) *Moment balance*

Assuming that body and surface couples are absent, we impose moment balance by requiring that †

$$\int_{\partial\mathcal{P}} (\boldsymbol{y}\times\boldsymbol{S}\boldsymbol{\nu}+\boldsymbol{n}\times\boldsymbol{\Sigma}\boldsymbol{\nu})\,da=\boldsymbol{0} \tag{3.7}$$

for all $\mathcal{P}$ and all time, or, equivalently, in view of (3.2) and (3.6), that

$$\boldsymbol{S}\boldsymbol{F}^{\top}+\boldsymbol{\Sigma}\boldsymbol{G}^{\top}+\boldsymbol{n}\otimes\boldsymbol{\pi}=(\boldsymbol{S}\boldsymbol{F}^{\top}+\boldsymbol{\Sigma}\boldsymbol{G}^{\top}+\boldsymbol{\pi}\otimes\boldsymbol{n})^{\top}, \tag{3.8}$$

on $\mathcal{R}$ for all time.

(*e*) *Dissipation imbalance*

We consider a purely mechanical situation where the first and second laws combine to yield a principle of dissipation imbalance and, introducing the energy density ψ, impose that imbalance by requiring that‡

$$\dot{\int_{\mathcal{P}}} \psi\,dv \le \int_{\partial\mathcal{P}} (\boldsymbol{S}\boldsymbol{\nu}\cdot\dot{\boldsymbol{y}}+\dot{q}\boldsymbol{\tau}\cdot\boldsymbol{\nu}+\boldsymbol{\Sigma}\boldsymbol{\nu}\cdot\dot{\boldsymbol{n}})\,da \tag{3.9}$$

for all $\mathcal{P}$ and all time, or, equivalently, in view of (3.2), (3.6), and (3.4), that

$$\dot{\psi}-\boldsymbol{S}\cdot\dot{\boldsymbol{F}}-\boldsymbol{\tau}\cdot\dot{\boldsymbol{h}}+k\dot{q}-\boldsymbol{\Sigma}\cdot\dot{\boldsymbol{G}}+\boldsymbol{\pi}\cdot\dot{\boldsymbol{n}}\le 0 \tag{3.10}$$

on $\mathcal{R}$ for all time.

4. Constitutive theory

For simplicity, we restrict our attention to constitutive relations of the form

$$\left.\begin{aligned}
\psi &= \hat{\psi}(\boldsymbol{F},q,\boldsymbol{h},\boldsymbol{n},\boldsymbol{G},\dot{q}),\\
\boldsymbol{S} &= \hat{\boldsymbol{S}}(\boldsymbol{F},q,\boldsymbol{h},\boldsymbol{n},\boldsymbol{G},\dot{q}),\\
\boldsymbol{\tau} &= \hat{\boldsymbol{\tau}}(\boldsymbol{F},\boldsymbol{n},\boldsymbol{G},q,\boldsymbol{h},\dot{q}),\\
k &= \hat{k}(\boldsymbol{F},q,\boldsymbol{h},\boldsymbol{n},\boldsymbol{G},\dot{q}),\\
\boldsymbol{\Sigma} &= \hat{\boldsymbol{\Sigma}}(\boldsymbol{F},q,\boldsymbol{h},\boldsymbol{n},\boldsymbol{G},\dot{q}),\\
\boldsymbol{\pi} &= \hat{\boldsymbol{\pi}}(\boldsymbol{F},q,\boldsymbol{h},\boldsymbol{n},\boldsymbol{G},\dot{q}),
\end{aligned}\right\} \tag{4.1}$$

with $\hat{\boldsymbol{S}}$, $\hat{\boldsymbol{\Sigma}}$, and $\hat{\boldsymbol{\pi}}$ defined consistent with the moment balance (3.8).

† In keeping with Anderson et al. (1999), only torques exerted by external agencies are accounted for in the moment balance.

‡ Using reasoning identical to that underlying the ommision of internal torques in (3.7), power expenditures associated with the internal orientational force density $\boldsymbol{\pi}$ and the internal aspherical force k are not included in (3.9).

(*a*) *Consequences of thermodynamics*

Employing the approach taken by Anderson et al. (1999), we find that the local dissipation imbalance (3.10) holds if and only if†

$$\left.\begin{aligned}
\psi &= \hat{\psi}(\boldsymbol{F}, q, \boldsymbol{h}, \boldsymbol{n}, \boldsymbol{G}),\\
\boldsymbol{S} &= \frac{\partial \hat{\psi}(\boldsymbol{F}, q, \boldsymbol{h}, \boldsymbol{n}, \boldsymbol{G})}{\partial \boldsymbol{F}} - p\boldsymbol{F}^{-\top},\\
\boldsymbol{\tau} &= \frac{\partial \hat{\psi}(\boldsymbol{F}, q, \boldsymbol{h}, \boldsymbol{n}, \boldsymbol{G})}{\partial \boldsymbol{h}},\\
k &= -\frac{\partial \hat{\psi}(\boldsymbol{F}, q, \boldsymbol{h}, \boldsymbol{n}, \boldsymbol{G})}{\partial q} - k_{\rm dis},\\
\boldsymbol{\Sigma} &= \frac{\partial \hat{\psi}(\boldsymbol{F}, q, \boldsymbol{h}, \boldsymbol{n}, \boldsymbol{G})}{\partial \boldsymbol{G}} + \boldsymbol{n}\otimes\boldsymbol{\chi},\\
\boldsymbol{\pi} &= -\frac{\partial \hat{\psi}(\boldsymbol{F}, q, \boldsymbol{h}, \boldsymbol{n}, \boldsymbol{G})}{\partial \boldsymbol{n}} + \lambda\boldsymbol{n} - \boldsymbol{G}\boldsymbol{\chi},
\end{aligned}\right\} \tag{4.2}$$

with p the constitutively indeterminate *pressure* required to maintain the constraint $\det \boldsymbol{F} = 1$, the dissipative contribution $k_{\rm dis} = \hat{k}_{\rm dis}(\boldsymbol{F}, \boldsymbol{n}, \boldsymbol{G}, q, \boldsymbol{h}, \dot{q})$ to the internal aspherical force density consistent with the residual inequality

$$\hat{k}_{\rm dis}(\boldsymbol{F}, \boldsymbol{n}, \boldsymbol{G}, q, \boldsymbol{h}, \dot{q})\dot{q} \leq 0, \tag{4.3}$$

and λ and $\boldsymbol{\chi}$ constitutively indeterminate *multiplier fields* required to maintain the constraint $|\boldsymbol{n}| = 1$ and its consequence $\boldsymbol{G}^{\top}\boldsymbol{n} = \boldsymbol{0}$.

Assuming that $\hat{k}_{\rm dis}$ varies smoothly with $\dot{q}$, (4.3) holds if and only if

$$k_{\rm dis} = -\beta\dot{q} \tag{4.4}$$

with

$$\beta = \hat{\beta}(\boldsymbol{F}, q, \boldsymbol{h}, \boldsymbol{n}, \boldsymbol{G}, \dot{q}) \geq 0 \tag{4.5}$$

the *drag coeffcient*.

Hence, within our framework, a complete constitutive description of a nematic elastomer consists of prescription of the free-energy density ψ and the drag coefficient β as functions of $(\boldsymbol{F}, q, \boldsymbol{h}, \boldsymbol{n}, \boldsymbol{G})$ and $(\boldsymbol{F}, q, \boldsymbol{h}, \boldsymbol{n}, \boldsymbol{G}, \dot{q})$, respectively.

(*b*) *Consequences of invariance and material symmetry*

To study the implications of invariance and material symmetry on the properties of $\hat{\psi}$ and $\hat{\beta}$, we suppress dependence on q and $\dot{q}$. Letting $\hat{f}$ denote either $\hat{\psi}$ or $\hat{\beta}$, we

† Throughout this work, partial derivatives with respect to $\boldsymbol{n}$ and $\boldsymbol{G}$ indicate differentiation on the manifold determined by the constraints $|\boldsymbol{n}| = 1$ and $\boldsymbol{G}^{\top}\boldsymbol{n} = \boldsymbol{0}$ (see Anderson et al. (1999)). The results (4.2) hinge on the presence of introduction of external forces that guarantee satisfaction of the balances (3.2), (3.6), and (3.4) in arbitrary processes.

enforce invariance with repsect to superposed rigid changes of observer by requiring that

$$\hat{f}(\boldsymbol{\Omega F}, \boldsymbol{h}, \boldsymbol{\Omega n}, \boldsymbol{\Omega G}) = \hat{f}(\boldsymbol{F}, \boldsymbol{h}, \boldsymbol{n}, \boldsymbol{G}) \tag{4.6}$$

for all rotations $\boldsymbol{\Omega}$.

Consistent with the assumption that the material be isotropic in the reference state, we postulate that, for all $\boldsymbol{\Lambda}$ with $\det \boldsymbol{\Lambda} = 1$,

$$\hat{f}(\boldsymbol{F\Lambda}, \boldsymbol{\Lambda}^{\top}\boldsymbol{h}, \boldsymbol{n}, \boldsymbol{G\Lambda}) = \hat{f}(\boldsymbol{F}, \boldsymbol{h}, \boldsymbol{n}, \boldsymbol{G}). \tag{4.7}$$

Combining (4.6) and (4.7), we find that

$$\hat{f}(\boldsymbol{F}, \boldsymbol{h}, \boldsymbol{n}, \boldsymbol{G}) = \tilde{f}(\boldsymbol{F}^{\top}\boldsymbol{F}, \boldsymbol{h}, \boldsymbol{F}^{\top}\boldsymbol{n}, \boldsymbol{F}^{\top}\boldsymbol{G}), \tag{4.8}$$

where $\tilde{f}$ is an isotropic function, viz.,

$$\tilde{f}(\boldsymbol{\Omega F}^{\top}\boldsymbol{F\Omega}^{\top}, \boldsymbol{\Omega}^{\top}\boldsymbol{h}, \boldsymbol{\Omega F}^{\top}\boldsymbol{n}, \boldsymbol{\Omega F}^{\top}\boldsymbol{G\Omega}^{\top}) = \tilde{f}(\boldsymbol{F}^{\top}\boldsymbol{F}, \boldsymbol{h}, \boldsymbol{F}^{\top}\boldsymbol{n}, \boldsymbol{F}^{\top}\boldsymbol{G}) \tag{4.9}$$

for all rotations $\boldsymbol{\Omega}$. Thus, on restoring dependence upon q and $\dot{q}$, it follows that invariance and material symmetry require that

$$\hat{\psi}(\boldsymbol{F}, q, \boldsymbol{h}, \boldsymbol{n}, \boldsymbol{G}) = \tilde{\psi}(\boldsymbol{F}^{\top}\boldsymbol{F}, q, \boldsymbol{h}, \boldsymbol{F}^{\top}\boldsymbol{n}, \boldsymbol{F}^{\top}\boldsymbol{G}) \tag{4.10}$$

and

$$\hat{\beta}(\boldsymbol{F}, q, \boldsymbol{h}, \boldsymbol{n}, \boldsymbol{G}, \dot{q}) = \tilde{\beta}(\boldsymbol{F}^{\top}\boldsymbol{F}, q, \boldsymbol{h}, \boldsymbol{F}^{\top}\boldsymbol{n}, \boldsymbol{F}^{\top}\boldsymbol{G}, \dot{q}), \tag{4.11}$$

with $\tilde{\psi}$ and $\tilde{\beta}$ isotropic scalar-valued functions of their arguments.

5. General governing equations

(*a*) *Deformational force balance*

Combining the local deformational force balance (3.2) and the constitutive relation $(4.2)_2$ for the deformational stress $\boldsymbol{S}$, we obtain the partial differential equation

$$\mathrm{Div}\Big(\frac{\partial\hat{\psi}(\boldsymbol{F}, \boldsymbol{n}, \boldsymbol{G}, q, \boldsymbol{h})}{\partial \boldsymbol{F}}\Big) = \boldsymbol{F}^{-\top}\mathrm{Grad}\, p. \tag{5.1}$$

(*b*) *Aspherical force balance*

Combining the local aspherical force balance (3.4) and the constitutive relations $(4.2)_{5,6}$ for the aspherical stress $\boldsymbol{\tau}$ and the internal aspherical force k, we obtain the partial differential equation

$$\mathrm{Div}\Big(\frac{\partial\hat{\psi}(\boldsymbol{F}, \boldsymbol{n}, \boldsymbol{G}, q, \boldsymbol{h})}{\partial \boldsymbol{h}}\Big) - \frac{\partial\hat{\psi}(\boldsymbol{F}, \boldsymbol{n}, \boldsymbol{G}, q, \boldsymbol{h})}{\partial q} = \hat{\beta}(\boldsymbol{F}, \boldsymbol{n}, \boldsymbol{G}, q, \boldsymbol{h}, \dot{q})\dot{q}. \tag{5.2}$$

(*c*) *Orientational force balance*

Combining the local orientational force balance (3.6) and the constitutive relations $(4.2)_{3,4}$ for the orientational stress $\boldsymbol{\Sigma}$ and the internal orientational force $\boldsymbol{\pi}$, we obtain the partial differential equation

$$\mathrm{Div}\Big(\frac{\partial\hat{\psi}(\boldsymbol{F},\boldsymbol{n},\boldsymbol{G},q,\boldsymbol{h})}{\partial\boldsymbol{G}}\Big)+(\mathrm{Div}\,\boldsymbol{\chi}+\lambda)\boldsymbol{n}=\frac{\partial\hat{\psi}(\boldsymbol{F},\boldsymbol{n},\boldsymbol{G},q,\boldsymbol{h})}{\partial\boldsymbol{n}}. \tag{5.3}$$

Since

$$\begin{aligned}(\boldsymbol{1}-\boldsymbol{n}\otimes\boldsymbol{n})&\mathrm{Div}\Big(\frac{\partial\hat{\psi}(\boldsymbol{F},\boldsymbol{n},\boldsymbol{G},q,\boldsymbol{h})}{\partial\boldsymbol{G}}\Big)\\&=\mathrm{Div}\Big(\frac{\partial\hat{\psi}(\boldsymbol{F},\boldsymbol{n},\boldsymbol{G},q,\boldsymbol{h})}{\partial\boldsymbol{G}}\Big)+\Big(\boldsymbol{G}\cdot\frac{\partial\hat{\psi}(\boldsymbol{F},\boldsymbol{n},\boldsymbol{G},q,\boldsymbol{h})}{\partial\boldsymbol{G}}\Big)\boldsymbol{n},\end{aligned} \tag{5.4}$$

(5.3) can be decomposed into components

$$\mathrm{Div}\Big(\frac{\partial\hat{\psi}(\boldsymbol{F},\boldsymbol{n},\boldsymbol{G},q,\boldsymbol{h})}{\partial\boldsymbol{G}}\Big)+\Big(\boldsymbol{G}\cdot\frac{\partial\hat{\psi}(\boldsymbol{F},\boldsymbol{n},\boldsymbol{G},q,\boldsymbol{h})}{\partial\boldsymbol{G}}\Big)\boldsymbol{n}=\frac{\partial\hat{\psi}(\boldsymbol{F},\boldsymbol{n},\boldsymbol{G},q,\boldsymbol{h})}{\partial\boldsymbol{n}} \tag{5.5}$$

and

$$\mathrm{Div}\,\boldsymbol{\chi}+\lambda=\boldsymbol{G}\cdot\frac{\partial\hat{\psi}(\boldsymbol{F},\boldsymbol{n},\boldsymbol{G},q,\boldsymbol{h})}{\partial\boldsymbol{G}} \tag{5.6}$$

perpendicular and parallel to $\boldsymbol{n}$. We interpret (5.6) as a restriction on the multiplier fields $\boldsymbol{\chi}$ and λ. As this restriction can be satisfied subsequent to the determination of $\boldsymbol{y}$, $\boldsymbol{n}$, and q, we remove (5.6) and the determination of $\boldsymbol{\chi}$ and λ from further consideration.

6. Particular constitutive equations

(*a*) *Free-energy density*

We now envision a situation where a nematic elastomer is formed in a two-step process. First, the melt is cross-linked in a uniaxial state with agglomeration

$$\boldsymbol{A}_*=(1+q_*)^{\frac{1}{3}}\Big(\boldsymbol{1}-\frac{q_*}{1+q_*}\boldsymbol{n}_*\otimes\boldsymbol{n}_*\Big),\qquad q_*>-1,\qquad|\boldsymbol{n}_*|=1. \tag{6.1}$$

Next, an annealing process is performed. This process randomizes the molecular orientation and results in an isotropic state ($q=0$)—taken to be our reference state—wherein the agglomeration at each material point is spherical. We assume the material "remembers" the extent of asphericity q_* present at the time of cross-linking. However, we suppose that the annealing process destroys any memory of the associated orientation $\boldsymbol{n}_*$.

To describe such a material, we consider a simplification and simultaneous extension of the molecular-statistical free-energy density of Warner, Gelling and Vilgis (1988). The simplification stems from taking the reference state to be isotropic and restricting the agglomeration to the uniaxial form (2.1). On the other hand,

the extension follows from accounting for energetic contributions associated with variations of the asphericity and orientation of the molecular agglomeration. The aspherical contribution includes a double-well potential in the asphericity and a term quadratic in the gradient of the asphericity. The double-well potential isolates as preferred the isotropic reference state and states with asphericity equivalent to that present at the time of cross-linking. The gradient term allows for the existence of equilibrium states in which the asphericity varies smoothly between its energetically preferred values. The orientational contribution involves two factors. Of these, one generalizes the OZF energy-density to account for deformation, while the other depends only on the asphericity in a manner designed to ensure integrability of the energy density when the orientation is undefined. Specifically, we assume that

$$\hat{\psi}(\boldsymbol{F},q,\boldsymbol{h},\boldsymbol{n},\boldsymbol{G}) = \frac{\mu}{2}\Big((1+q)^{\frac{1}{3}}\Big(|\boldsymbol{F}|^2 - \frac{q}{1+q}|\boldsymbol{F}^{\top}\boldsymbol{n}|^2\Big) - 3\Big) + \Phi(q) + \frac{\alpha}{2}|\boldsymbol{h}|^2 + \Gamma(q)K(\boldsymbol{F},\boldsymbol{n},\boldsymbol{G}), \quad (6.2)$$

with $\mu > 0$ the *rubber-elasticity modulus*, Φ, a double-well potential, consistent with

$$\left.\begin{aligned} \Phi(q_*) = \Phi(0) = 0, \\ \Phi(q) > 0 \quad \text{for } q \neq q_*, 0, \\ \Phi(q) \to +\infty \quad \text{as } q \to -1, +\infty, \end{aligned}\right\} \quad (6.3)$$

$\alpha > 0$ a *regularizing modulus*, Γ, a mollifying factor, dimensionless and consistent with

$$\left.\begin{aligned} \Gamma(q) = O(q^2) \quad \text{as } q \to 0, \\ \Gamma(q) > 0 \quad \text{for } q \neq 0, \\ \Gamma(q) \to +\infty \quad \text{as } q \to -1, +\infty, \end{aligned}\right\} \quad (6.4)$$

and generalization

$$K(\boldsymbol{F},\boldsymbol{n},\boldsymbol{G}) = \kappa_1(\boldsymbol{F}\cdot\boldsymbol{G})^2 + \kappa_2|\boldsymbol{F}^{\top}\boldsymbol{G}|^2 + \kappa_3(\boldsymbol{F}^{\top}\boldsymbol{G})\cdot(\boldsymbol{G}^{\top}\boldsymbol{F}) + \kappa_4(|\boldsymbol{F}^{\top}\boldsymbol{G}\boldsymbol{F}^{\top}\boldsymbol{n}|^2 + |\boldsymbol{G}^{\top}\boldsymbol{F}\boldsymbol{F}^{\top}\boldsymbol{n}|^2) + \kappa_5(\boldsymbol{F}^{\top}\boldsymbol{G}\boldsymbol{F}^{\top}\boldsymbol{n})\cdot(\boldsymbol{G}^{\top}\boldsymbol{F}\boldsymbol{F}^{\top}\boldsymbol{n}) \quad (6.5)$$

of the OZF energy-density, involving *orientational-elasticity moduli* $\kappa_1 > 0$, $\kappa_2 > 0$, $\kappa_3 > 0$, $\kappa_4 > 0$, and $\kappa_5 > 0$. On setting $\boldsymbol{F} = \boldsymbol{1}$ in (6.5), we may identify $\kappa_1+\kappa_2+\kappa_4$, κ_2, $\kappa_2+\kappa_3$, and $\kappa_2+\kappa_4$ with the classical splay, twist, bend, and saddle-splay moduli of the OZF theory; $\kappa_4+\kappa_5$ is an additional saddle-splay modulus that accounts for interactions between the distortion of network cross-links and the orientation of the molecular agglomeration. Both Ψ and Γ penalize states in which the asphericity limits toward the extreme values $q = -1$ and $q = \infty$.

(*b*) *Drag coefficient*

For simplicity, we take the drag coefficient to be a positive constant, viz.,

$$\hat{\beta}(\boldsymbol{F},\boldsymbol{n},\boldsymbol{G},q,\boldsymbol{h},\dot{q}) = \beta = \text{constant} > 0. \quad (6.6)$$

7. Extension of a cylindrical specimen

We now use the theory to investigate whether a disclination may form in a right circular cylinder subjected to an isochoric extension. We ignore time-dependence; thus, in particular, $\dot{q} = 0$. Therefore, we will obtain information concerning the existence of disclinations but not about their generation or subequent evolution.

(*a*) *Preliminaries*

We consider a specimen that, in the reference state, occupies the right circular-cylinder

$$\mathcal{R} = \{\boldsymbol{x} = r\boldsymbol{e}_r + z\boldsymbol{e}_z : 0 \leq r < R, -\infty < z < \infty\}, \tag{7.1}$$

with cylindrical coordinates (r, θ, z) and $\{\boldsymbol{e}_r, \boldsymbol{e}_\theta, \boldsymbol{e}_z\}$ the associated physical basis.

We stipulate that the deformation have the form

$$\boldsymbol{y}(r, \theta, z) = Ar\boldsymbol{e}_r + \frac{z}{A^2}\boldsymbol{e}_z, \qquad \text{with} \quad 0 < A < 1, \tag{7.2}$$

for all (r, θ, z) in $\mathcal{R}$, so that the cylinder is extended along its axis. From (7.2),

$$\boldsymbol{F}(r, \theta, z) = A(\boldsymbol{1} - \boldsymbol{e}_z \otimes \boldsymbol{e}_z) + \frac{1}{A^2}\boldsymbol{e}_z \otimes \boldsymbol{e}_z, \tag{7.3}$$

for all (r, θ, z) in $\mathcal{R}$, and a direct calculation shows that the constraint (2.4) holds for all (r, θ, z) in $\mathcal{R}$.

As our interest is in whether the deformation creates a state involving a disclination of strength $+1$ along the axis of the specimen, we assume that, except when the material is isotropic (i.e., when $q = 0$),

$$\boldsymbol{n}(r, \theta, z) = \boldsymbol{e}_r \tag{7.4}$$

and, accordingly,

$$\boldsymbol{G}(r, \theta, z) = \frac{1}{r}\boldsymbol{e}_\theta \otimes \boldsymbol{e}_\theta \tag{7.5}$$

for all (r, θ, z) in $\mathcal{R}$.

Further, we assume that the asphericity is independent of θ and z, viz.,

$$q(r, \theta, z) = q(r). \tag{7.6}$$

(*b*) *Deformational force balance*

Using the particular form for $\hat{\psi}$ in (6.2) and specializing to reflect the kinematical assumptions (7.3), (7.4), and (7.6), we find that

$$\frac{\partial \hat{\psi}(\boldsymbol{F}, \boldsymbol{n}, \boldsymbol{G}, q, \boldsymbol{h})}{\partial \boldsymbol{F}} = \frac{\mu A}{(1+q)^{\frac{2}{3}}}(\boldsymbol{1} - \boldsymbol{e}_z \otimes \boldsymbol{e}_z) + \frac{\mu(1+q)^{\frac{1}{3}}}{A^2}\boldsymbol{e}_z \otimes \boldsymbol{e}_z + A\Big(\frac{\mu q}{(1+q)^{\frac{2}{3}}} + \frac{\kappa \Gamma(q)}{r^2}\Big)\boldsymbol{e}_\theta \otimes \boldsymbol{e}_\theta, \tag{7.7}$$

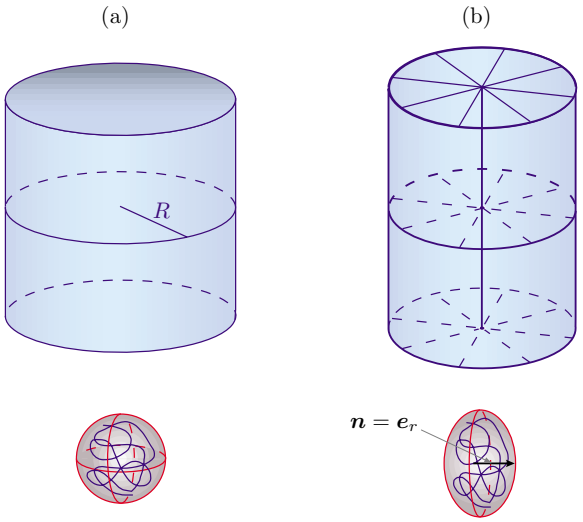

Figure 1. The cylinder and the molecular conformation in: (a) the reference state; (b) the distorted state, with an axial disclination of strength +1.

where

$$\kappa = \kappa_1 + \kappa_2 + \kappa_3 \tag{7.8}$$

is the *orientational-splay modulus*.†

Then, using (7.7) in the deformational force balance (5.1), we arrive at the partial-differential equation

$$\Big(\mu\Big(\frac{d}{dr}\Big(\frac{1}{(1+q)^{\frac{2}{3}}}\Big) - \frac{q}{r(1+q)^{\frac{2}{3}}}\Big) - \frac{\kappa\Gamma(q)}{r^3}\Big)\boldsymbol{e}_r \\ = \frac{1}{A^2}\frac{\partial p}{\partial r}\boldsymbol{e}_r + \frac{1}{A^2 r}\frac{\partial p}{\partial \theta}\boldsymbol{e}_\theta + A\frac{\partial p}{\partial z}\boldsymbol{e}_z, \tag{7.9}$$

which must hold on $\mathcal{R}$. Further, we require that the lateral surface of the cylinder be free of deformational traction, viz., $\boldsymbol{S}\boldsymbol{e}_r = \boldsymbol{0}$ when $r = R$, whereby

$$\Big(\frac{\mu A}{(1+q)^{\frac{2}{3}}} - \frac{p}{A}\Big)\Big|_{r=R} = 0. \tag{7.10}$$

In view of the angular and axial components of (7.9), it follows that the pressure is independent of θ and z; further, using the radial component of (7.9) and (7.10), we find that

$$p(r) = \frac{\mu A^2}{(1+q(r))^{\frac{2}{3}}} + \mu A^2 \int_r^R \frac{q(\xi)\,d\xi}{\xi(1+q(\xi))^{\frac{2}{3}}} + \kappa A^2 \int_r^R \frac{\Gamma(q(\xi))\,d\xi}{\xi^3}. \tag{7.11}$$

Thus, with knowledge of the asphericity, the pressure is determined completely.

† See the discussion following (6.5).

(*c*) *Aspherical force balance*

Using the particular form (6.2) for $\hat{\psi}$ and specializing to reflect the kinematical assumptions (7.3), (7.4), and (7.6), straightforward calculations show that

$$\frac{\partial\hat{\psi}(\boldsymbol{F},\boldsymbol{n},\boldsymbol{G},q,\boldsymbol{h})}{\partial\boldsymbol{h}}=\alpha\frac{\partial q}{\partial r}\boldsymbol{e}_r. \tag{7.12}$$

and

$$\frac{\partial\hat{\psi}(\boldsymbol{F},\boldsymbol{n},\boldsymbol{G},q,\boldsymbol{h})}{\partial q}=\frac{\mu A^2}{6(1+q)^{\frac{2}{3}}}\Big(\frac{1}{A^6}-\frac{1-q}{1+q}\Big)+\frac{\kappa A^2\Gamma'(q)}{r^2}+\Phi'(q). \tag{7.13}$$

Then, using (7.12) and (7.13) in the aspherical force balance (5.2), we arrive at the ordinary-differential equation

$$\frac{\alpha}{r}\frac{d}{dr}\Big(r\frac{dq}{dr}\Big)=\frac{\mu A^2}{6(1+q)^{\frac{2}{3}}}\Big(\frac{1}{A^6}-\frac{1-q}{1+q}\Big)+\frac{\kappa A^2\Gamma'(q)}{r^2}+\Phi'(q), \tag{7.14}$$

which holds on $(0,R)$.

In addition, we require that the specimen be free of aspherical traction on the lateral surface of the cylinder as well as on the cylinder axis, viz., $\boldsymbol{\tau}\cdot\boldsymbol{e}_r=0$ when $r=0$ and $r=R$, which yields the boundary conditions

$$\alpha\frac{\partial q}{\partial r}\Big|_{r=0}=\alpha\frac{\partial q}{\partial r}\Big|_{r=R}=0. \tag{7.15}$$

(*d*) *Orientational force balance*

Using the particular form (6.2) for $\hat{\psi}$ and specializing to reflect the kinematical assumptions (7.3), (7.4) and (7.6), we find that, except when the material is isotropic,

$$\frac{\partial\hat{\psi}(\boldsymbol{F},\boldsymbol{n},\boldsymbol{G},q,\boldsymbol{h})}{\partial\boldsymbol{G}}=\frac{\kappa A^2\Gamma(q)}{r}\boldsymbol{e}_\theta\otimes\boldsymbol{e}_\theta \tag{7.16}$$

where κ is the orientational-splay modulus defined in (7.8), and

$$\frac{\partial\hat{\psi}(\boldsymbol{F},\boldsymbol{n},\boldsymbol{G},q,\boldsymbol{h})}{\partial\boldsymbol{n}}=\boldsymbol{0}. \tag{7.17}$$

Thus,

$$\mathrm{Div}\Big(\frac{\partial\hat{\psi}(\boldsymbol{F},\boldsymbol{n},\boldsymbol{G},q,\boldsymbol{h})}{\partial\boldsymbol{n}}\Big)=-\frac{\kappa A^2\Gamma(q)}{r^2}\boldsymbol{e}_r=-\Big(\boldsymbol{G}\cdot\frac{\partial\hat{\psi}(\boldsymbol{F},\boldsymbol{n},\boldsymbol{G},q,\boldsymbol{h})}{\partial\boldsymbol{G}}\Big)\boldsymbol{n} \tag{7.18}$$

and the balance (5.5) is satisfied trivially wherever the material is anisotropic.

(*e*) *Scaling*

We take the maximum height of the barrier separating the minima of the double-well potential Φ to be proportional to ν. Introducing $x=r/R$ and $Q(x)=q(Rx)$, we obtain the dimensionless groups

$$\mu^*=\frac{\mu}{\nu},\qquad \kappa^*=\frac{\kappa}{R^2\nu},\qquad \text{and}\qquad \alpha^*=\frac{\alpha}{R^2\nu}, \tag{7.19}$$

and define

$$\Psi = \frac{\psi}{\nu}, \quad \boldsymbol{T} = \frac{1}{\nu}(\boldsymbol{S} + p\boldsymbol{F}^{-\top}), \quad P = \frac{p}{\nu}, \quad \text{and} \quad \boldsymbol{\Upsilon} = \frac{1}{R\nu}(\boldsymbol{\Sigma} - \boldsymbol{n}\otimes\boldsymbol{\chi}). \tag{7.20}$$

In view of the kinematical assumptions (7.3), (7.4), and (7.6), we find that

$$\Psi = \frac{\mu^*}{2}\Big((1+Q)^{\frac{1}{3}}\Big(A^2\Big(\frac{2+Q}{1+Q}\Big) + \frac{1}{A^4}\Big) - 3\Big) + \frac{\kappa^* A^2 \Gamma(Q)}{2x^2} + \frac{\Phi(Q)}{\nu} + \frac{\alpha^*}{2}\Big(\frac{dQ}{dx}\Big)^2, \tag{7.21}$$

that $\boldsymbol{T} = T_{xx}\boldsymbol{e}_r\otimes\boldsymbol{e}_r + T_{\theta\theta}\boldsymbol{e}_\theta\otimes\boldsymbol{e}_\theta + T_{zz}\boldsymbol{e}_z\otimes\boldsymbol{e}_z$, with

$$\left.\begin{aligned} T_{xx} &= \frac{\mu^* A}{(1+Q)^{\frac{2}{3}}}, \\ T_{\theta\theta} &= \mu^* A(1+Q)^{\frac{2}{3}} + \frac{\kappa^* A \Gamma(Q)}{x^2}, \\ T_{zz} &= \frac{\mu^*(1+Q)^{\frac{1}{3}}}{A^2}, \end{aligned}\right\} \tag{7.22}$$

that

$$P = \frac{\mu^* A^2}{(1+Q)^{\frac{2}{3}}} + \mu^* A^2 I_1 + \kappa^* A^2 I_2, \tag{7.23}$$

with

$$I_1(x) = \int_x^1 \frac{Q(\xi)\,d\xi}{\xi(1+Q(\xi))^{\frac{2}{3}}} \qquad \text{and} \qquad I_2(x) = \int_x^1 \frac{\Gamma(Q(\xi))\,d\xi}{\xi^3}, \tag{7.24}$$

and that $\boldsymbol{\Upsilon} = \Upsilon_{\theta\theta}\boldsymbol{e}_\theta\otimes\boldsymbol{e}_\theta$, with

$$\Upsilon_{\theta\theta} = \frac{\kappa^* A^2 \Gamma(Q)}{x}. \tag{7.25}$$

We find it useful to express Ψ as a sum

$$\Psi = \Psi_e + \Psi_a + \Psi_o, \tag{7.26}$$

with

$$\Psi_e = \frac{\mu^*}{2}\Big(2A^2 + \frac{1}{A^4} - 3\Big) \tag{7.27}$$

a conventional neo-Hookean rubber-elastic contribution associated with the distortion of network cross-links,

$$\Psi_a = \frac{\mu^*}{2}\Big(A^2\Big(\frac{2+Q}{(1+Q)^{\frac{2}{3}}} - 2\Big) + \frac{1}{A^4}\big((1+Q)^{\frac{1}{3}} - 1\big)\Big) + \frac{\Phi(Q)}{\nu} + \frac{\alpha^*}{2}\Big(\frac{dQ}{dx}\Big)^2 \tag{7.28}$$

a contribution associated with the asphericity of the molecular agglomeration, and

$$\Psi_o = \frac{\kappa^* A^2 \Gamma(Q)}{2x^2} \tag{7.29}$$

a contribution associated with the axis about which the molecular agglomeration is oriented.

Applying the scaling to (7.14) and (7.15), we find that the dimensionless asphericity is governed by the ordinary-differential equation

$$\frac{\alpha^*}{x}\frac{d}{dx}\Big(x\frac{dQ}{dx}\Big) = \frac{\mu^* A^2}{6(1+Q)^{\frac{2}{3}}}\Big(\frac{1}{A^6} - \frac{1-Q}{1+Q}\Big) + \frac{\kappa^* A^2 \Gamma'(Q)}{x^2} + \frac{\Phi'(Q)}{\nu} \tag{7.30}$$

and boundary conditions

$$\alpha^* \frac{dQ}{dx}\Big|_{x=0} = \alpha^* \frac{dQ}{dx}\Big|_{x=1} = 0. \tag{7.31}$$

(*f*) *Numerical results*

The differential equation (7.30) involves functions Φ and Γ, which are restricted only by (6.3) and (6.4). For our numerical investigation, we took

$$\Phi(q) = \frac{\nu q^2 (q-q_*)^2}{2(1+q)^2}, \tag{7.32}$$

where, as stated before, $\nu > 0$ determines the height of the energy barrier between states with $q = 0$ and $q = q_*$, and

$$\Gamma(q) = \begin{cases} \dfrac{q^2}{2(1+q)^2} & \text{if } -1 < q \le 0, \\[2ex] \dfrac{q^2}{2} & \text{if } q \ge 0. \end{cases} \tag{7.33}$$

While defined piecewise, this choice of Γ is twice continuously-differentiable. Thus, since (7.30) involves only the first derivative of Γ, we expect no numerical difficulties to ensue from this choice.

Since the deformation in (7.2) is restricted to extension ($0 < A < 1$), we expect an elongation of the molecular agglomeration parallel to the cylinder axis during extension. Thus, it is natural to restrict q_* to lie between -1 and 0. Otherwise, there would be no reason for a disclination to form. However, considering the case of cylinder compression ($A > 1$), the molecular agglomeration would be prolate in the radial direction, and we would therefore choose $q_* > 0$.

Using (7.32), we solved the boundary-value problem (7.30)–(7.31) numerically from $x = 0$ to $x = 1$ using the ACDC package of Cash and Wright (1998) with the tolerance on the solution of Q set to 10^{-8} and that of its derivative dQ/dx set to 10^{-4}. In so doing, we chose $\mu = \nu = 10^5$ J/m^3, $\kappa = \alpha = 10^{-11}$ J/m, and $R = 1$ cm. The values of μ and κ are realistic and in line with previous work (Warner and Terentjev 1996). As a result of these choices, $\mu^* = 1$ and $\kappa^* = \alpha^* = 10^{-12}$. Further, for illustrative purposes, we took $q_* = -0.3$. As our initial, trial solution, we used the straight line $Q = 0$, satisfying (7.31) and consisting of 501 evenly spaced points on the closed domain. The only parameter varied was A, the degree of cylinder extension, which we allowed to range between 0.86 and 1. Figure 4 shows a sharp transition between isotropic ($q = 0$) and anisotropic ($q \neq 0$) regions along the cylinder radius, thereby indicating the presence of a disclination. The extent of the

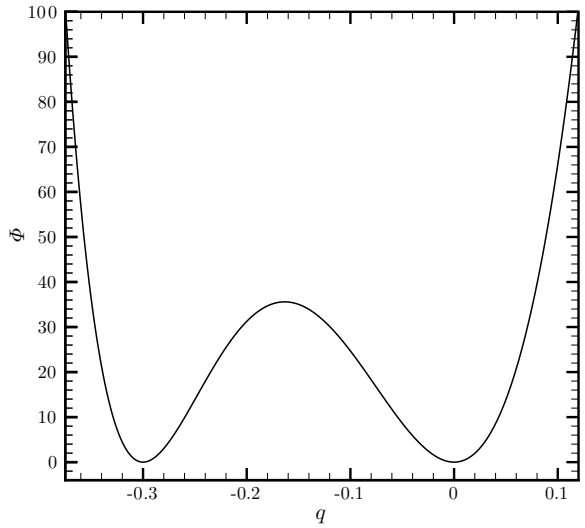

Figure 2. Plot of Φ, as defined in (7.32) for $\nu = 10^5$ J/m^3 and $q_* = -0.3$.

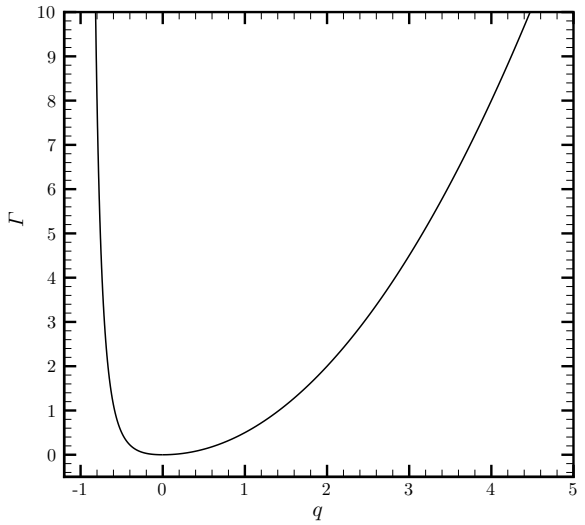

Figure 3. Plot of Γ, as defined in (7.33).

disclination core can also be inferred from the plot as the region where Q exhibits a rapid decrease (Mottram and Hogan 1997). From Figure 4, the center of the transition zone appears to be at $x = 10^{-6}$, which corresponds to a dimensional core radius on the order of 10^{-2} μm and is consistent with the length scale predicted by the ratio $\sqrt{\kappa/\mu} = \sqrt{\kappa/\nu}$ for our choices of μ, ν, and κ. A closer examination of the solution curves places the center of the layer at $x = 1.5 \times 10^{-6}$ (corresponding to a core radius of 0.015 μm), which we associate with the core boundary and denote by x_c. Our core radius is of the same order as values observed for liquid crystalline melts (Chandrasekhar and Ranganath 1986).

For each A, the contributions, Ψ_e and $\Psi - \Psi_o$, to the dimensionless free-energy

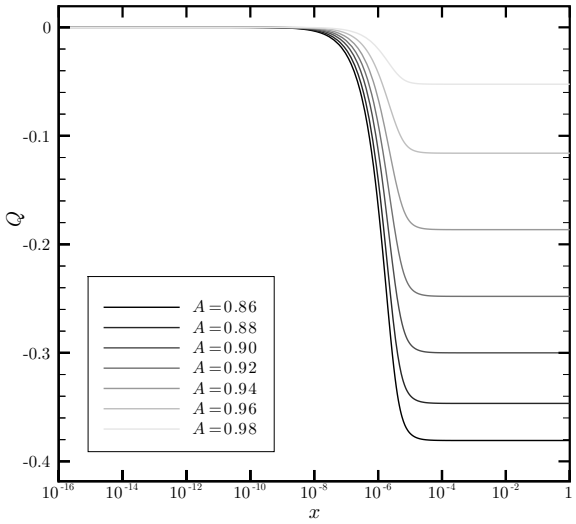

Figure 4. Plots of the asphericity Q as a function of dimensionless radial position x (note logarithmic scale) for the dimensionless material parameters $\mu^* = 1$, $\kappa^* = \alpha^* = 10^{-12}$, and $q_* = -0.3$ and representative values of the degree A of cylinder distortion between 0.86 and 1. Consistent with (7.31), note the horizontal slopes at the cylinder center ($x = 0$) and outer boundary ($x = 1$). A state connecting the energetically preferred values 0 and q_* of the asphericity is generated for $A \approx 0.90$.

density of (7.26) are both unassociated with the axis of orientation of the molecular agglomeration and are shown in Figure 5. The difference, $\Psi - \Psi_e$, which includes all terms of (7.26) unrelated to the neo-Hookean distortion of the network cross-links is plotted in Figure 6. We see from Figures 5 and 6 that the free-energy density has a markedly different behavior below and above x_c. This confirms our initial estimate of the core region from Figure 4. From Figure 5, Ψ_e is constant across the entire domain, while for corresponding values of extension, $\Psi - \Psi_o$ is greater than Ψ_e inside the core but less without. We note that the difference between Ψ_e and $\Psi - \Psi_o$ increases with greater extension away from the core. In the same region, we see from Figure 6 that $\Psi - \Psi_e$ decreases with increasing extension. Taken together and noting that the core is only a small part of the domain, these trends presage that the total neo-Hookean energy

$$\mathcal{F}_e^{\rm tot} = \int_0^1 \Psi_e(x)\, dx \tag{7.34}$$

will always be greater than the total energy

$$\mathcal{F}^{\rm tot} = \int_0^1 \Psi(x)\, dx \tag{7.35}$$

and that their difference will grow with increasing extension.

In fact, the free-energy totals $\mathcal{F}_e^{\rm tot}$ and $\mathcal{F}^{\rm tot}$ shown in Figure 7 do indeed bear this out. We note an expected monotonic increase of both $\mathcal{F}_e^{\rm tot}$ and $\mathcal{F}^{\rm tot}$ with increasing cylinder elongation (decreasing A). Also, as we surmised earlier, for all extension ratios, $\mathcal{F}^{\rm tot}$ is less than $\mathcal{F}_e^{\rm tot}$, the isotropic ($Q = 0$) neo-Hookean contribution alone.

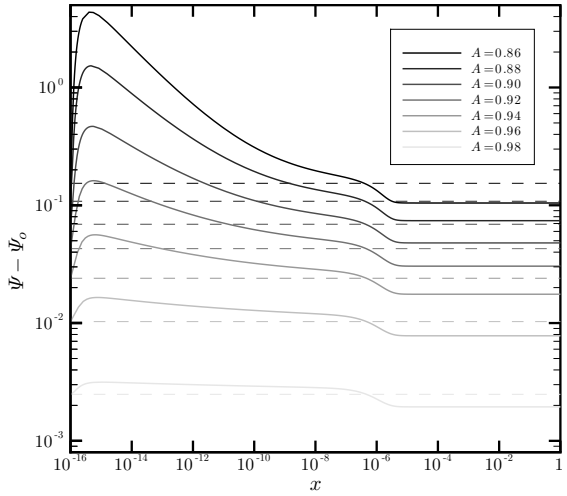

Figure 5. Plots of the contributions of $\Psi - \Psi_o$ (solid lines) and Ψ_e (dashed lines) to the free-energy density as a function of dimensionless radial position x (note logarithmic scale) for the dimensionless material parameters $\mu^* = 1$, $\kappa^* = \alpha^* = 10^{-12}$, and $q_* = -0.3$ and representative values of the degree A of cylinder distortion between 0.86 and 1.

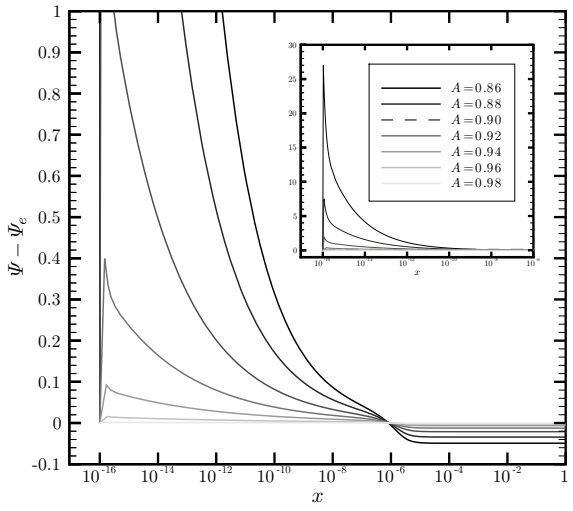

Figure 6. Plots of the portion $\Psi - \Psi_e$ of the free-energy density, excluding the elastic contribution, as a function of dimensionless radial position x (note logarithmic scale) for the dimensionless material parameters $\mu^* = 1$, $\kappa^* = \alpha^* = 10^{-12}$, and $q_* = -0.3$ and representative values of the degree A of cylinder distortion between 0.86 and 1.

From Figure 4, all extensions give rise to a non-trivial asphericity at $x \gtrsim 10^{-6}$. Therefore, the results from Figure 7 show that for any extension ratio, there is an energetic motivation for the material not to remain isotropic but to form a disclinated region with the remainder of the domain in an anisotropic state. This

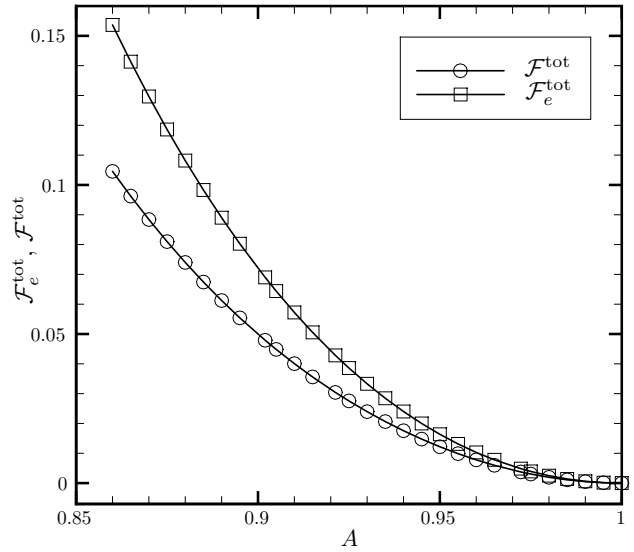

Figure 7. Plots of the total neo-Hookean rubber-elastic energy $\mathcal{F}_e^{\rm tot}$ and of the total free-energy $\mathcal{F}^{\rm tot}$ as a function of the degree A of cylinder distortion between 0.86 and 1 for the dimensionless material parameters $\mu^* = 1$, $\kappa^* = \alpha^* = 10^{-12}$, and $q_* = -0.3$.

incentive becomes stronger as the extension increases, as indicated by the growth of $\mathcal{F}_e^{\rm tot} - \mathcal{F}^{\rm tot}$ with extension shown in Figure 7. The lack of a threshold value of extension below which the isotropic state is preferred and above which a disclinated one is favored can be attributed to the fact that the well heights of Φ in Figure 2 are equal. If the well corresponding to $q = 0$ were lower than that for $q = q_*$ we would expect a threshold, with extent depending on the height difference between the wells. On the other hand, a threshold would still be absent if the well corresponding to $q = 0$ were higher than that for $q = q_*$.

In addition, we investigated the energy of the core, which we denote as

$$\mathcal{F}^{\rm core} = \int_0^{x_c} \Psi(x)\, dx, \tag{7.36}$$

relative to that of the whole domain. From Figure 8, it is evident that $\mathcal{F}^{\rm core}$ is a vanishingly small percentage of $\mathcal{F}^{\rm tot}$. This is because of the relatively small size of the core and the fact that Ψ_e is of a comparatively large magnitude across the entire domain. However, we see that the core becomes energetically more important with increasing extension for most of our range until $A \approx 0.875$. For greater values of extension ($A \lesssim 0.875$), the core becomes energetically less important as more energy goes into both stretching of the network cross-links and changing the asphericity of the molecules comprising the network.

The non-trivial components T_{xx}, $T_{\theta\theta}$, and T_{zz} of the constitutively determined contribution to the dimensionless deformational stress are shown in Figures 9–11, the dimensionless pressure P in Figure 12, and the non-trivial component $\Upsilon_{\theta\theta}$ of the constitutively determined contribution to the dimensionless orientational stress in Figure 13. We note from (7.22) that when $Q = 0$, T_{xx}, $T_{\theta\theta}$, and T_{zz} collapse to the conventional neo-Hookean expression. An interesting characteristic of T_{xx}

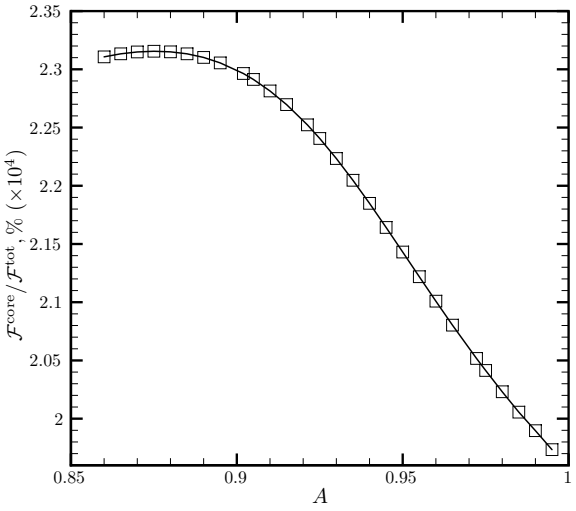

Figure 8. Plot of the percentage $\mathcal{F}^{\rm core}/\mathcal{F}^{\rm tot}$ of free energy in the core as a function of the degree A of cylinder distortion between 0.86 and 1 for the dimensionless material parameters $\mu^* = 1$, $\kappa^* = \alpha^* = 10^{-12}$, and $q_* = -0.3$.

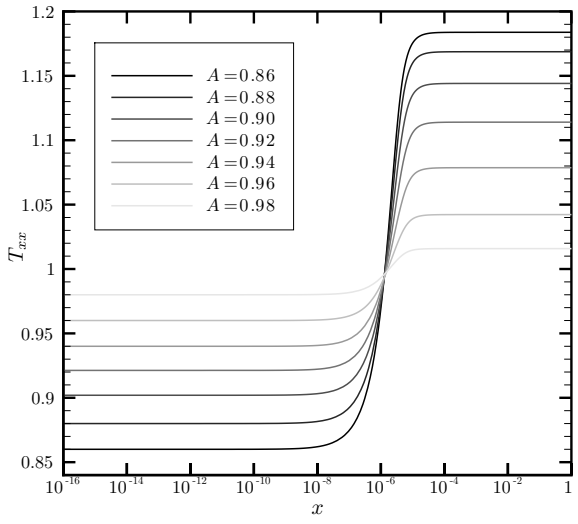

Figure 9. Plot of the radial component T_{xx} of the deformational stress as a function of dimensionless radial position x (note logarithmic scale) for the dimensionless material parameters $\mu^* = 1$, $\kappa^* = \alpha^* = 10^{-12}$, and $q_* = -0.3$ and representative values of the degree A of cylinder distortion between 0.86 and 1.

can be discerned from Figure 9. Here, the standard pattern of a higher stress for a greater extension ratio is inverted within the core. Thus, the radial component of deformational stress within the core descreases with increased stretching. This is consistent with neo-Hookean behavior since from Figure 4, $Q = 0$ within the core.

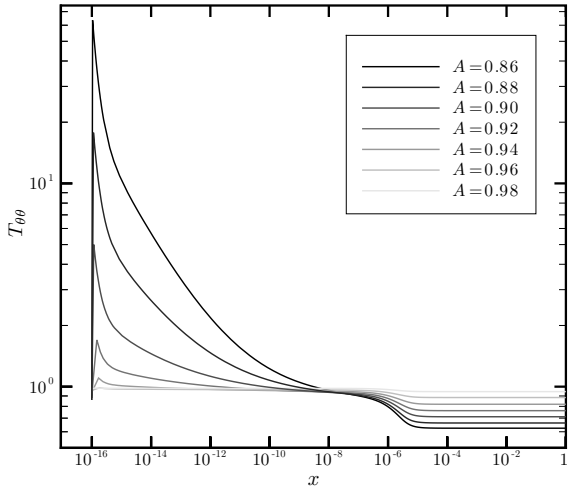

Figure 10. Plot of the hoop component $T_{\theta\theta}$ of the deformational stress as a function of dimensionless radial position x (note logarithmic scale) for the dimensionless material parameters $\mu^* = 1$, $\kappa^* = \alpha^* = 10^{-12}$, and $q_* = -0.3$ and representative values of the degree A of cylinder distortion between 0.86 and 1.

So, in the core $T_{xx} = \mu^* A$, and a greater extension (lower A) results in a lower stress. Outside the core though, more extension gives rise to higher stresses. This is contrary to the neo-Hookean trend within the core and is due to the fact that $Q < 0$ there. Since Q becomes more negative with increasing extension (see Figure 4) and because of the nature in which it appears in $(7.22)_1$, it makes sense that T_{xx} grows with extension away from the core. Like T_{xx}, the dimensionless hoop stress, $T_{\theta\theta}$, in Figure 10 shows a distinct transition at the core boundary but exhibits behavior antipodal to that of T_{xx}. So, $T_{\theta\theta}$ is much larger inside the core than without, with greater extension resulting in higher stress in the core but reduced stress in the rest of the domain. As for T_{xx}, inside the core, the first term of $T_{\theta\theta}$ in $(7.22)_2$ has a neo-Hookean character because $Q = 0$ there. However, this is overshadowed by the sharp peak, similar to that exhibited by $\Psi - \Psi_e$ in Figure 6, of $T_{\theta\theta}$ within the core. The cause of this behavior is identical in both cases and due to Ψ_o in (7.29), a component of $\Psi - \Psi_e$ and proportional to the second term of $T_{\theta\theta}$ in $(7.22)_2$. In fact, combining (7.29) and $(7.22)_2$ gives $T_{\theta\theta} = \mu^* A(1 + Q(x))^{\frac{2}{3}} + 2\Psi_o$. Outside of the core though, as Q becomes more negative and x greater, $T_{\theta\theta}$ is reduced from its neo-Hookean value. This reduction is greater for lower Q and upon consulting Figure 4, explains why $T_{\theta\theta}$ is lower for greater extension (lower A). From Figure 11, we observe that within the core, where $Q = 0$, the variation of T_{zz} with x is neo-Hookean. Then, away from the core, where the asphericity becomes negative (Figure 4), and as a result of the $(1 + Q)^{\frac{1}{3}}$ factor, T_{zz} assumes values less than the corresponding ones for the neo-Hookean case. Since the square of the extension ratio appears in the denominator of $(7.22)_3$, the stress grows for increasing extension.

The dimensionless pressure P defined in (7.23) is shown in Figure 12. For each A, P reaches a maximum at the cylinder center ($x = 0$) and decreases monotonically until attaining its minimum at the core boundary ($x = x_c$). Then, it monotonically

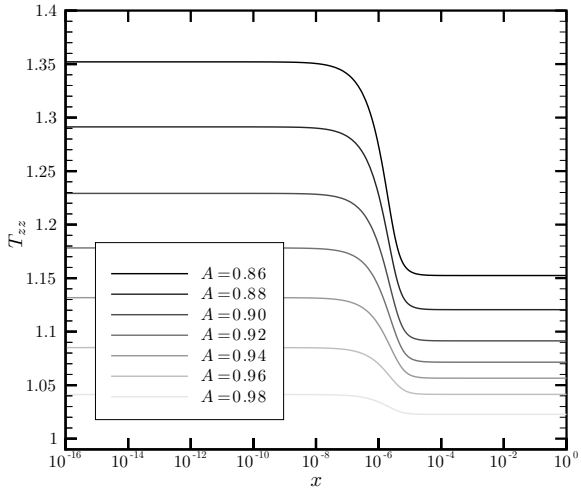

Figure 11. Plot of the axial component, T_{zz}, of the deformational stress as a function of dimensionless radial position x (note logarithmic scale) for the dimensionless material parameters $\mu^* = 1$, $\kappa^* = \alpha^* = 10^{-12}$, and $q_* = -0.3$ and representative values of the degree A of cylinder distortion between 0.86 and 1.

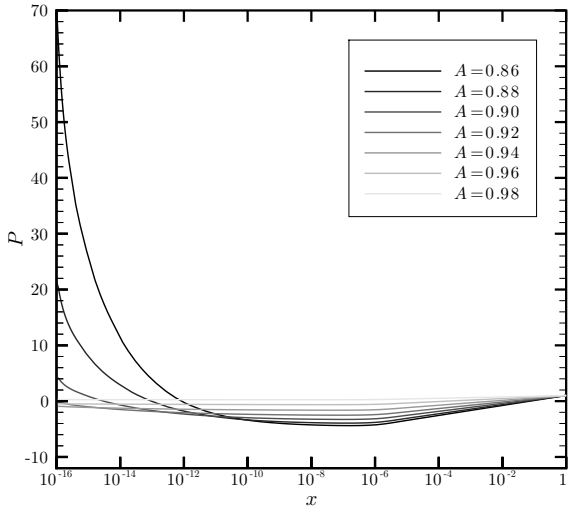

Figure 12. Plot of the dimensionless pressure P as a function of dimensionless radial position x (note logarithmic scale) for the dimensionless material parameters $\mu^* = 1$, $\kappa^* = \alpha^* = 10^{-12}$, and $q_* = -0.3$ and representative values of the degree A of cylinder distortion between 0.86 and 1.

increases until the edge of the cylinder, where it reaches almost the same value regardless of A. This is because the last two terms of (7.23) vanish at $x = 1$, so that the pressure at the edge is only dependent on the first term, which is essentially constant over our range of A. Although small in absolute terms, from Figure 13,

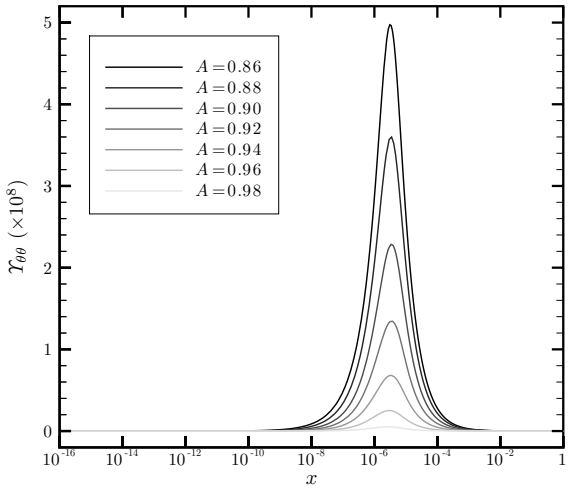

Figure 13. Plot of the hoop component, $\Upsilon_{\theta\theta}$, of the orientational stress as a function of dimensionless radial position x (note logarithmic scale) for the dimensionless material parameters $\mu^* = 1$, $\kappa^* = \alpha^* = 10^{-12}$, and $q_* = -0.3$ and representative values of the degree A of cylinder distortion between 0.86 and 1.

we see that $\Upsilon_{\theta\theta}$ is concentrated entirely about $x = x_c$. Greater $\Upsilon_{\theta\theta}$ for increased extension is due to the presence of Γ (see Figure 3) in (7.25) and the trend of Q in Figure 4.

8. Discussion

As with any important class of new materials such as nematic elastomers, to proceed with applications designed to take complete advantage of their unique properties, a thorough theoretical understanding of their behavior is necessary. In this spirit and working within a rigorous theoretical framework, we predict the existence of disclinations in nematic elastomers for the first time. We also obtain information concerning the characteristic dimension of a disclination core and the distributions of energy, deformational stress, pressure, and orientational stress in disclinated states. We show that there is an energetic reason for the material to become disclinated as opposed to remaining isotropic as would a conventional neo-Hookean rubber. Since disclinations have been found to be so important in conventional liquid crystals, it is also likely that this will be the case in nematic elastomers. While our predictions are confined to nematic elastomers which have been specially prepared, we speculate that disclinations may occur under other circumstances. We hope that this work leads to further study in this area and, especially, to experiments designed to test our predictions.

Acknowledgments

This work was supported by the National Science Foundation and the Department of Energy.

References

Adrienko, D., Allen, M.P., 2000. Molecular simulation and theory of a liquid crystalline disclination core. *Physical Review E* **61** 1, 504–510.

Anderson, D. R., Carlson, D. E., Fried, E., 1999. A continuum-mechanical theory for nematic elastomers. *J. Elasticity* **56**, 33–58.

Cash, J. R., Wright, R. W., 1998. Continuous extensions of deferred correction schemes for the numerical solution of nonlinear two-point boundary value problems. *Appl. Numer. Math.* **28**, 227–244.

Chandrasekhar, S., 1988. Recent developments in the physics of liquid crystals. *Contemp. Phys.* **29** 6, 527–558 (1988).

Chandrasekhar, S., Ranganath, G. S., 1986. The structure and energetics of defects in liquid crystals. *Adv. Phys.* **35**, 507–596.

Davis, F. J., 1993. Liquid-crystalline elastomers. J. Mater. Chem. **3** 6, 551–562.

DeSimone A., Dolzmann, G., 2000. Material instabilities in nematic elastomers. *Physica D* **136**, 175–191.

Ericksen, J. L., 1991. Liquid-crystals with variable degree of orientation. *Arch. Rat. Mech. Anal.* **113** 2, 97–120.

Finkelmann, H., Kim, S. T., Munoz, A., Palffy-Muhoray, P., Taheri, B., 2001. Tunable Mirrorless Lasing in Cholesteric Liquid Crystalline Elastomers. *Advanced Materials* **13** 14.

Frank, F. C., 1958. On the theory of liquid crystals. *Discussions of the Faraday Society* **25**, 19–28.

Kléman, M. Defects in liquid crystals. *Rep. Prog. Phys.* **52**, 555-654 (1989).

Mottram, N. J., Hogan, S. J., 1997. Disclination core structure and induced phase change in nematic liquid crystals. *Phil. Trans. R. Soc. Lond. A* **355**, 2045–2064.

Mottram, N. J., Sluckin, T. J., 2000. Defect-induced melting in nematic liquid crystals. *Liquid Crystals* **27** 10, 1301–1304.

Oseen, W. C., 1933. The theory of liquid crystals. *Transactions of the Faraday Society* **29** 883–899.

Warner, M., Terentjev, E. M., 1996. Nematic elastomers—A new state of matter. *Prog. Polym. Sci.* **21**, 853–891.

Warner, M. Gelling, K. P., Vilgis, T. A., 1988. Theory of nematic networks. *Journal of Chemical Physics* **88** 4008–4013.

Williams, C., Pierański, P.. Cladis, P. E., 1972. Nonsingular $S = +1$ screw disclination lines in nematics. *Phys. Rev. Lett.* **29** 2, 90–92.

Zentel, R., 1989. Liquid crystalline elastomers. *Angew. Chem. Adv. Mater.* **101** 10, 1437–1445.

Zöcher, H., 1933. The effect of a magnetic field on the nematic state. *Transactions of the Faraday Society* **29** 945–957.